



Experimental overview on small collision systems at the LHC

Constantin Loizides

Lawrence Berkeley National Laboratory, Berkeley, California, USA

Abstract

These conferences proceedings summarize the experimental findings obtained in small collision systems at the LHC, as presented in the special session on “QGP in small systems?” at the Quark Matter 2015 conference. (The arXiv version is significantly longer than the printed proceedings, with more details and a short discussion.)

Keywords: heavy-ion, collectivity, high multiplicity, QGP

1. Introduction

Key evidence for the formation of a hot Quark-Gluon Plasma (QGP) in nucleus–nucleus (AA) collisions at high collision energies is the presence of jet quenching [1] and bulk collective effects [2], together with their absence in proton–nucleus (pA) or deuteron–gold (dAu) control experiments [3]. The control measurements are needed to characterize the extent to which initial-state effects can be differentiated from effects due to final-state interactions in the QGP [4]. It is assumed that initial-state physics can be isolated since the QGP, if at all produced in such light–heavy ion reactions, is expected to be tenuous.

Indeed, in the case of hard processes at mid-rapidity, control experiments, both at RHIC in dAu collisions at $\sqrt{s_{NN}} = 200$ GeV [5–8], and at the LHC in pPb collisions at $\sqrt{s_{NN}} = 5.02$ TeV [9–24], demonstrated the absence of strong final state effects. In particular, the minimum bias pPb data can be well described by superimposing $N_{\text{coll}} = A\sigma_{\text{pp}}/\sigma_{\text{pPb}} \approx 7$ independent pp collisions with only small modifications induced by the initial state or cold nuclear matter.

However, measurements of multi-particle correlations over large pseudorapidity (η) range in high multiplicity pPb events [25–29] exhibit remarkable similarities with results related to collective effects from PbPb collisions at $\sqrt{s_{NN}} = 2.76$ TeV [30].¹ In fact, soon after the start of the LHC program in 2010, a pronounced longitudinal structure in the two-dimensional angular correlation function measured for particle pairs over azimuthal angle and η differences, $\Delta\varphi$ and $\Delta\eta$, with transverse momentum (p_T) of 1–3 GeV/c was observed in high-multiplicity pp events at 7 TeV [31]. The appearance of these “ridge-like” structures in high-multiplicity pp and pA events caused speculation of similar physics being at work in these small collision systems. In particular, there is an ongoing debate as to whether they are of common hydrodynamic origin [32], or created already by strong correlations in the initial state from gluon saturation [33].

In these QM15 proceedings, following the presentation at the conference [34], a summary on experimental results from small collision systems at the LHC with an emphasis on bulk properties will be given.

¹Similar effects had been observed already at RHIC in dAu collisions [35], but were ignored until the LHC data were reported. For a summary of the recent experimental results at RHIC, see Ref. [36].

Observable or effect	PbPb	pPb (at high mult.)	pp (at high mult.)	Refs.
Low p_T spectra (“radial flow”)	yes	yes	yes	[37–42]
Intermed. p_T (“recombination”)	yes	yes	yes	[41–47]
Particle ratios	GC level	GC level except Ω	GC level except Ω	[48–51]
Statistical model	$\gamma_s^{\text{GC}} = 1, 10\text{--}30\%$	$\gamma_s^{\text{GC}} \approx 1, 20\text{--}40\%$	$\gamma_s^{\text{C}} < 1, 20\text{--}40\%$ ²	[52]
HBT radii ($R(k_T), R(\sqrt[3]{N_{\text{ch}}})$)	$R_{\text{out}}/R_{\text{side}} \approx 1$ ³	$R_{\text{out}}/R_{\text{side}} \lesssim 1$	$R_{\text{out}}/R_{\text{side}} \lesssim 1$	[53–59]
Azimuthal anisotropy (v_n) (from two part. correlations)	$v_1 - v_7$	$v_1 - v_5$	v_2, v_3	[25–27] [60–67]
Characteristic mass dependence	v_2, v_3 ⁴	v_2, v_3	v_2	[67–73]
Directed flow (from spectators)	yes	no	no	[74]
Higher order cumulants (mainly $v_2\{n\}, n \geq 4$)	“ $4 \approx 6 \approx 8 \approx \text{LYZ}$ ” +higher harmonics	“ $4 \approx 6 \approx 8 \approx \text{LYZ}$ ” +higher harmonics	“ $4 \approx 6$ ” ⁵	[28, 29, 67] [75–83]
Weak η dependence	yes	yes	not measured	[83–90]
Factorization breaking	yes ($n = 2, 3$)	yes ($n = 2, 3$)	not measured	[91]
Event-by-event v_n distributions	$n = 2 - 4$	not measured	not measured	[92]
Event plane and v_n correlations	yes	not measured	not measured	[93–95]
Direct photons at low p_T	yes	not measured	not measured ⁶	[96]
Jet quenching	yes	not observed ⁷	not measured ⁸	[97–105]
Heavy flavor anisotropy	yes	hint ⁹	not measured	[106–109]
Quarkonia	$J/\psi \uparrow, \Upsilon \downarrow$	suppressed	not measured ⁸	[110–116]

Table 1. Summary of observables or effects (classified as known from AA data) in PbPb collisions, as well as in high multiplicity pPb and pp collisions at the LHC. References to key measurements for the various observables and systems are given. See text for details.

2. Summary of observations in PbPb collisions

In order to classify the observed phenomena in small systems, it is useful to briefly discuss the conclusions drawn from observations in PbPb collisions at the LHC, as compiled in Table 1. Particle ratios and yields are described as a Grand Canonical ensemble by the statistical model with the strangeness under-saturation factor $\gamma_s \approx 1$ and with only moderate deviations of 10–30% from thermal yields [51, 52]. Almost all particles (with $p_T \lesssim 2$ GeV/c) can be described by hydrodynamics, which efficiently translates initial spatial anisotropies (ε_i) into final momentum anisotropies (v_i) assuming that the pressure gradients have built up early in the evolution of the system [123]. Hydrodynamic models quantitatively describe “average observables” as radial flow [37, 38] and the transverse momentum (p_T) and pseudorapidity (η) dependence of the azimuthal anisotropies v_n [60–63, 75–77, 84–86], as well as their characteristic mass dependence [68–71]. Furthermore, hydrodynamic calculations can also (at least qualitatively) capture “higher order” details, such as the breaking of factorization due to event-plane angle decorrelations in p_T and η [91], v_n distributions [92], as well as event-plane angle and event-by-event v_n correlations across different harmonics [93–95]. Approximately describing direct photon production at low p_T , such models determine the initial temperature

²Statistical model results were extracted only for minimum-bias pp data.

³The dependence of the freeze-out parameters relative to the event-plane angle has also been measured [117].

⁴Identified particle $v_2\{4\}$ from cumulants has also been measured [118].

⁵Attempts to measure $v_2\{4\}$ in pp from cumulants before 2015 did not extract a real (non-imaginary) value for v_2 [73, 119].

⁶A measurement in minimum bias pp collisions at 7 TeV is consistent with zero at low p_T [120].

⁷Jet quenching has not been directly observed [121], but in analogy with PbPb (where v_2 at high p_T is thought to be caused by path-length dependent energy loss), the possible non-zero v_2 at large p_T may be indicative of parton energy loss in pPb [64].

⁸Conceptually, it is not straightforward to measure a modification because of difficulties to define a rigorous normalization for nuclear effects, which is already a challenge in the case of pA collisions due to the contribution from multiple-parton interactions [121].

⁹There are long-range two-particle correlation measurements of heavy-flavor electron–hadron correlations at mid-rapidity [122] and inclusive muon–hadron correlations at forward rapidity [88], which may be indicative of non-zero v_2 for heavy-flavor particles.

of the QGP to exceed about 400 MeV in central collisions [96]. The freeze-out radii in 3 orthogonal directions (“out”, “side”, “long”) can be deduced from measurements of quantum-statistics correlations between pairs of same-charge pions (HBT) at low momentum transfer. The radii are found to scale with $\sqrt[3]{N_{\text{ch}}}$ (indicating a constant density at freeze-out) and to decrease with increasing pair momentum (k_T) as expected from hydrodynamics [53]. The size along the emission direction is similar to the geometric size of the system ($R_{\text{out}}/R_{\text{side}} \approx 1$). Directed flow, both the rapidity-odd as well as the rapidity-even components, of charged particles at mid-rapidity was measured relative to the collision symmetry plane defined by the spectator nucleons, and evidence for dipole-like initial density fluctuations in the overlap region was found [74]. At intermediate p_T ($2 \lesssim p_T \lesssim 5$ GeV/ c), the yield of heavier particles is enhanced relative to that of lighter particles [43–45], an effect typically described by calculations employing a combination of hydrodynamics and quark coalescence (or recombination) [124]. The created system is opaque for high- p_T colored probes, which due to radiational and collisional energy loss (jet quenching) are strongly suppressed [97–105], and transparent for photons and other colorless probes, which roughly scale with N_{coll} [125–131]. Jet quenching leads to slightly modified jet fragmentation functions inside small jet cone sizes ($R = 0.4$) [132, 133], and most of the radiated energy appears at large angles ($R > 0.8$) [99, 134]. Due to interactions and rescattering with the medium, even heavy-flavor particles exhibit finite anisotropies [106–109]. Strong support for the formation of a deconfined medium with color degrees of freedom is the relative enhancement of J/ψ yields, in particular at low p_T , due to statistical recombination or regeneration [110, 111], and the sequential suppression of Υ states [112].

In summary, the system created in high-energy PbPb collisions at the LHC exhibits features expected for strongly-interacting partonic matter. There are a few outstanding problems, such as the small p/π ratio [37], the non-zero elliptic flow measured for direct photons [135], the rather large v_3 relative to v_2 measured in ultra-central PbPb collisions [136], and the significant suppression of three- and four-pion Bose-Einstein correlations compared to expectations from two-pion measurements [137]. These problems will need to be resolved in the future, but are not expected to invalidate the general conclusions outlined above.

3. Results from pPb collisions at high multiplicity

Table 1 compares results from measurements in PbPb collisions, discussed in the previous section, with those in high multiplicity pPb collisions, where available. As in PbPb collisions, the p_T spectra of identified particles harden with increasing multiplicity [39, 41, 42] and, if interpreted in the same way as in PbPb collisions (using a blast wave model fit) reveal, even larger radial flow than in PbPb events with similar multiplicity as predicted [138]. With increasing multiplicity, particle ratios reach the grand canonical level except for the Ω particle, which however gets near [49, 50]. Nevertheless, at high multiplicity, the yields can be described by the statistical model with $\gamma_S \approx 1$ and with deviations of 20–40% (only slightly worse than in the case of PbPb) from the thermal expectation [52]. At first, long-range ($2 < |\Delta\eta| < 4$) ridge structures on the near side ($\Delta\varphi \approx 0$) were measured using two-particle angular correlations in high multiplicity pPb collisions [25], and found to have a much larger strength than that of similar long range structures in high-multiplicity pp collisions at 7 TeV [31]. Later, azimuthal anisotropy coefficients v_2 and v_3 were extracted from per-trigger yields measured over azimuthal angle and η differences, $\Delta\varphi$ and $\Delta\eta$, respectively [26, 27]. The per-trigger yields obtained in low multiplicity events (which were shown to be similar to pp collisions at 2.76 and 7 TeV) were subtracted, in order to suppress the dominant background from jets. Soon after, genuine four-particle correlations were also measured [28, 29], where the contribution from two-particle correlations were systematically removed (referred to as the “cumulant method” [139]). The multiplicity and p_T dependencies of v_2 and v_3 turned out to be similar to those obtained in PbPb collisions provoking speculations about the same physical origin in both systems [30]. Recently, cumulant measurements have been extended to genuine six- and eight-particle correlations, as well as the Lee Yang Zero (LYZ) method, which is conceptually equivalent to measuring the correlation of all particles [140]. As in PbPb collisions, it was found that, within 10%, $v_2\{4\} \approx v_2\{6\} \approx v_2\{8\} \approx v_2\{\text{LYZ}\}$ in high multiplicity pPb collisions [81], as shown in Fig. 1. The presence of non-zero higher-order cumulants with similar magnitude, and in particular with a finite and similar value for $v_2\{\text{LYZ}\}$ can be interpreted as crucial evidence for a hydrodynamically evolving system, where all particles, and hence the single-particle distribution itself, would be correlated

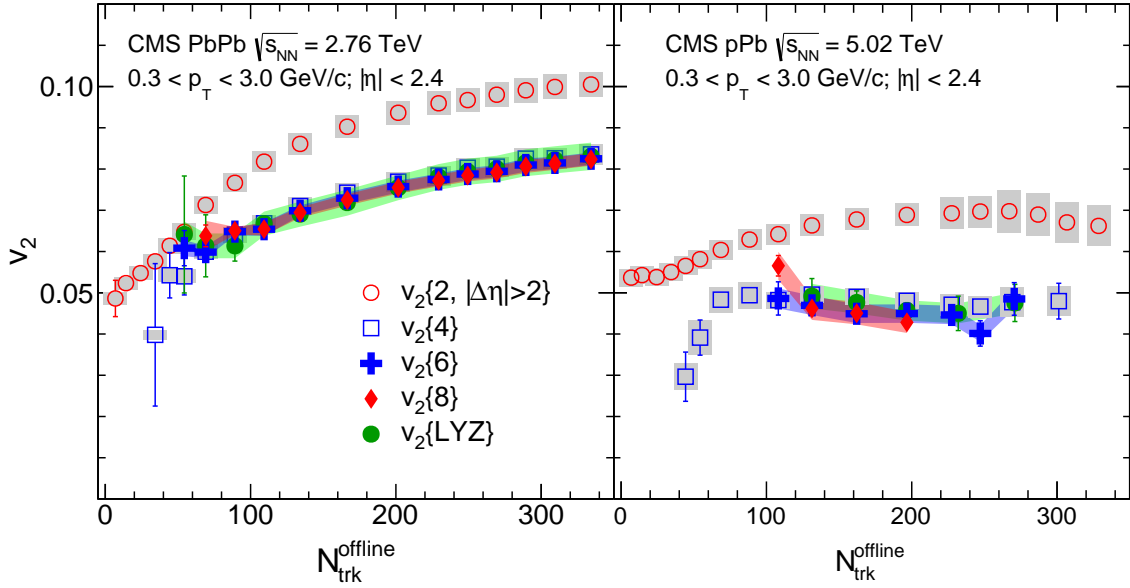


Fig. 1. The multiplicity dependence of $v_2\{n\}$ for $n = 2, 4, 6, 8$ and $v_2\{\text{LYZ}\}$ averaged over $0.3 < p_T < 3$ GeV/c, for PbPb (left) and pPb (right panel) collisions. Figure taken from Ref. [81].

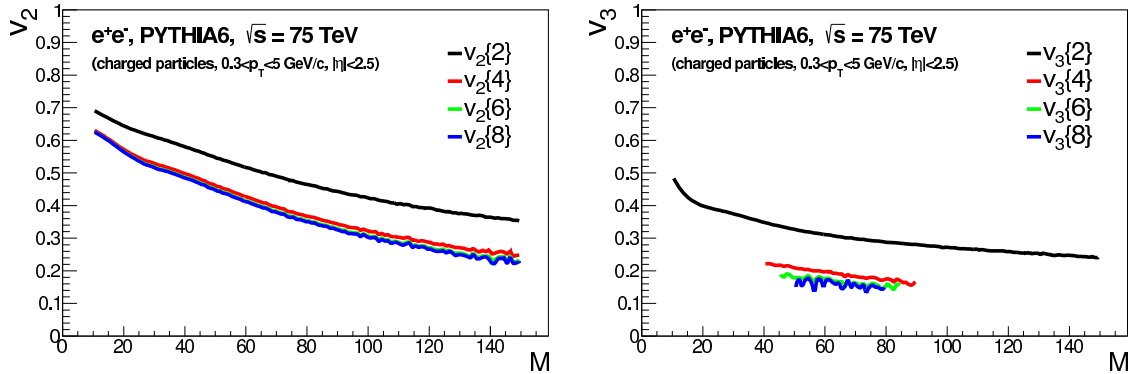


Fig. 2. Second (left panel) and third (right panel) harmonics extracted from 2-, 4-, 6- and 8-particle cumulants vs charged particle multiplicity (M) in e^+e^- collisions generated with PYTHIA (v6.425) at $\sqrt{s} = 75$ TeV. Charged particles with $0.3 < p_T < 5$ GeV/c and within $|\eta| < 2.5$ are used in the calculation. For v_3 , the higher-order results could only be reliably extracted in a limited range of M .

to the initial-state symmetry planes. However, there are also arguments in disfavor of this interpretation. Firstly, higher-order cumulants can have similar values even though the underlying correlations originate from a different mechanism than hydrodynamics. This is demonstrated in Fig. 2 by comparing various multi-particle cumulants extracted for e^+e^- collisions generated with the PYTHIA event generator [141]. However, such apparent collectivity is a trivial consequence if the number of sources for particle production is just a few. Secondly, in case of a narrow underlying distribution of v_2 (where the width is significantly smaller than the mean), the higher moments generally only differ by parametrically small amounts [142]. Thirdly, models based on only quantum chromodynamics, and not involving hydrodynamics, which do not require final-state interactions among quarks and gluons, have also been suggested to explain the observed multi-particle correlations, but have not provided any quantitative predictions yet [143, 144]. However, the v_2 and v_3 coefficients also exhibit a similar mass dependence as in PbPb [71, 72], with the v_2 and v_3 for

heavier particle being depleted at low p_T , and the protons and Λ crossing the v_2 (and v_3) of pions and neutral kaons, respectively, between p_T of 1.5–3 GeV/ c . In PbPb, the same effect is generally accepted to be a robust prediction of hydrodynamics, caused by the interplay of radial flow with the higher harmonics at lower p_T [145] and recombination at higher p_T [124], affected also by the presence of a dense hadron gas at later stages of the collision evolution. The breaking of factorization due to η and p_T dependent event-plane angle fluctuations is also found to be similar between pPb and PbPb collisions [91]. As in PbPb, a rather weak η dependence for v_2 and v_3 is measured [83, 87–89], in particular when the results are corrected for a possible effect arising from event-plane angle decorrelation along η . Also, similarly to PbPb, HBT radii are found to scale with $\sqrt[3]{N_{\text{ch}}}$, to decrease with increasing k_T , and $R_{\text{out}}/R_{\text{side}}$ approaches ≈ 1 at low k_T [55, 56, 58, 59]. In the intermediate p_T range ($2 \lesssim p_T \lesssim 5$ GeV/ c), the spectra of identified particles show a characteristic enhancement in pPb compared to pp collisions (scaled by $N_{\text{coll}} \approx 7$) [46, 47], often referred to as ‘‘Cronin’’ enhancement. In the same p_T region, particle ratios of p/π and Λ/K_S^0 show an enhancement also, whose magnitudes increase and maxima shift to higher p_T with increasing multiplicity, depicting a similar p_T dependence to PbPb collisions [42, 45].

The results discussed so far are reported in intervals of multiplicity measured either at mid- or forward rapidity, generally called ‘‘event activity classes’’. To ensure that the conclusions are qualitatively robust against variation of the event selection, the measurements are sometimes reported for several different event activity definitions. Quantitative interpretation of the data requires, however, that one takes into account that the observable and event activity may be correlated by the complex interplay between hard, multiple semi-hard and soft processes. This correlation is suspected to induce strong changes of high-energy jet [146], dijet [147], D-meson [148] and Υ production [113] with event activity. In order to compare data with calculations addressing nuclear effects, event activity classes have also been related to an estimate of the number of collisions (or participants with $N_{\text{part}} = N_{\text{coll}} + 1$ in pPb) via a Glauber model [121, 149]. Due to the ordering of events according to their activity, pPb events with more than average activity per nucleon–nucleon collision populate the higher multiplicity classes, while with less than average activity the lower multiplicity classes [150]. The event selection bias leads to a large variation of the nuclear modification factor, $Q_{\text{pPb}} = 1/N_{\text{coll}} Y_{\text{pPb}}/Y_{\text{pp}}$, and complicates a direct measurement of nuclear modification [121]¹⁰. Nevertheless, by comparing the data with a superposition of PYTHIA pp events, in which the event activity selection is performed in the same as in the data, it can be deduced that Q_{pPb} for charged particles, when integrated over 10 to 20 GeV/ c , is not significantly altered by the nuclear environment. This conclusion is supported by a different approach, where events are ordered based on the zero-degree energy of slow neutrons produced in the collision on the Pb-going side, and an estimate of N_{coll} from a data-driven approach inspired by the wounded nucleon model [121]. Furthermore, no significant nuclear modification has been seen in (charged) jet spectra [152], D-meson yields [148] nor dijet k_T [153] at mid-rapidity either. While direct jet quenching [154] has not been observed, possible non-zero v_2 values of about 5% at p_T up to 10 GeV/ c albeit with rather large uncertainty have been reported [64]. In analogy to PbPb (where v_2 at high p_T is thought to be caused by path-length dependent energy loss), this observation may be a hint of parton energy loss in pPb. However, the effect can also be qualitatively described by initial-state gluon correlations without (collective) final state interactions [155]. At forward rapidities, there are hints of final-state effects reported in the multiplicity dependence of J/ψ Q_{pPb} [115] and in the observed suppression of $\psi(2S)$ relative to J/ψ [114, 116]. Lastly, there also are long-range two-particle correlation measurements of heavy-flavor electron–hadron correlations at mid-rapidity [122] and inclusive muon–hadron correlations at forward rapidity [88], both revealing a double-ridge structure, which may be indicative of non-zero v_2 for heavy-flavor particles.

¹⁰High- p_T related results measured in minbias pPb collisions at mid-rapidity [9–24], mentioned in Sec. 1, do not have this problem. The charged particle R_{pPb} at high p_T is consistent with unity. Initial discrepancies between results from ALICE, ATLAS and CMS, are now identified to be related to the interpolated pp reference [151], and final confirmation can be expected from the analysis of pp collisions at $\sqrt{s} = 5.02$ TeV taken end of 2015.

4. Results from pp collisions at high multiplicity

Table 1 compares results from measurements in PbPb and pPb collisions, discussed in the previous sections, with those in high multiplicity pp collisions, where available. Identified particle spectra at low p_T show the same characteristic features as in pPb collisions, in particular a significant hardening with increasing multiplicity [40, 41]. Furthermore, at intermediate p_T ($2 \lesssim p_T \lesssim 5$ GeV/c) particle ratios of p/π and Λ/K_S^0 show a similar enhancement as in pPb collisions [41, 45, 48]. The data are consistent with the interpretation of strong radial flow developed in high multiplicity pp collisions [156]. Alternatively, however, microscopic effects such as the Color Reconnection (CR) mechanism of strings implemented in PYTHIA can also qualitatively explain the data [157]. PYTHIA with CR describes the increase of the average p_T with multiplicity [158] and the multiplicity dependence of charge-dependent correlations (balance function) [159] quite well. Measured particle ratios increase with increasing multiplicity in the same way as in pPb collisions [48]. The statistical model has so far only been applied to minimum bias pp collisions and, when treated as a canonical ensemble, was found to describe the yields with $\gamma_s^C < 1$ and deviations of only about 20–40% from the expected yields [52]. HBT radii show the same trends with N_{ch} and k_T as in pPb collisions, and at high multiplicity R_{out}/R_{side} approaches ≈ 1 at low k_T [55, 57, 58], consistent with the interpretation of collective flow [160].

At the same multiplicity, near-side ridge yields extracted from long-range two-particle angular correlations at 13 TeV [161] agree with those measured at 7 TeV [31], while they are a factor of 10 and 4 smaller than in PbPb and pPb collisions, respectively. In pp even more so than in pPb collisions, jets are the dominant source of two-particle correlations, and in order to extract the long-range Fourier coefficients their contribution to the long-range correlations needs to be subtracted first. Thus, as for the pPb results, the per-trigger yield measured at low multiplicity scaled by a factor F is subtracted from that measured at high multiplicity, before the Fourier coefficients (A_n) from the long-range $\Delta\eta$ projection are computed. Finally, the two-particle Fourier coefficients $V_n = A_n/B$ are obtained by normalizing the Fourier coefficients relative to the baseline (B) extracted in the high multiplicity events (usually denoted with capital letters to distinguish them from those of the single-particle azimuthal distribution denoted with lower letters). The single-particle Fourier coefficients are then $v_n = \sqrt{V_n}^{11}$. The factor F can be obtained in various ways, for example as ratio of the short-range near-side yield in high multiplicity to that in low multiplicity events after the long-range $\Delta\eta$ contributions have been subtracted. Assuming that the away-side jet shape per-trigger yields do not significantly change with multiplicity, the long-range jet contribution to the per-trigger yields should be significantly reduced. In this way, significant (p_T integrated) v_2 and v_3 coefficients have recently been reported in high multiplicity (M)¹²pp collisions [65, 73], with values of about 5% and 1%, respectively, about 30% and 50% smaller than in pPb at similar multiplicity. The p_T dependence of v_2 is found to be independent of M above $M \gtrsim 75$, and independent of collision energy (from 2.76 to 13 TeV).¹³Below $M \lesssim 70$, v_2 decreases with decreasing multiplicity. Interestingly in this region, an ambiguity in the precise determination of v_2 arises [65] as the extracted v_2 values are found to depend on the number of tracks used to define the low-multiplicity event sample (see right panel of Fig. 3, where the effect is shown in the case of ATLAS' template fit method further mentioned below). Larger v_2 are extracted with event classes, which are defined with even smaller multiplicity of only up to 10 and 5 tracks, respectively. The cause for the dependence of v_2 on the choice of the low multiplicity event class is not yet clear. It could originate from diffractive processes, or string breaking and resonance decay effects, which contribute to the correlation, since quite low p_T particles are included in the measurement. Both effects may significantly influence the

¹¹In case different p_T ranges are used for trigger and associated particles, they are usually computed by relying on factorization $V_n(p_T^1, p_T^2) = v_n(p_T^1)v_n(p_T^2)$, which is found to approximately hold by selecting different p_T ranges for associated particles

¹²Multiplicity is given as the number of reconstructed charged tracks with $p_T > 0.4$ GeV/c in $|\eta| < 2.4$ for CMS and $p_T > 0.5$ GeV/c in $\eta < 2.5$ for ATLAS. To roughly account for the tracking inefficiency scale by 1.2, and by 1.5 to extrapolate to $p_T = 0$. Hence $M = 100$ approximately corresponds to 5–6 times the average multiplicity in pp, and is similar to the charged particle density at mid-rapidity of 70–80% PbPb and 20–25% CuCu collisions at $\sqrt{s_{NN}} = 2.76$ TeV and $\sqrt{s_{NN}} = 200$ GeV, respectively [162, 163].

¹³The integrated v_2 can not easily be compared between the ATLAS and CMS results as ATLAS uses $0.5 < p_T < 5$ while CMS $0.3 < p_T < 3$ GeV/c. However, within (quite large) systematic uncertainties the p_T -differential measurements of ATLAS and CMS agree, as shown in [34].

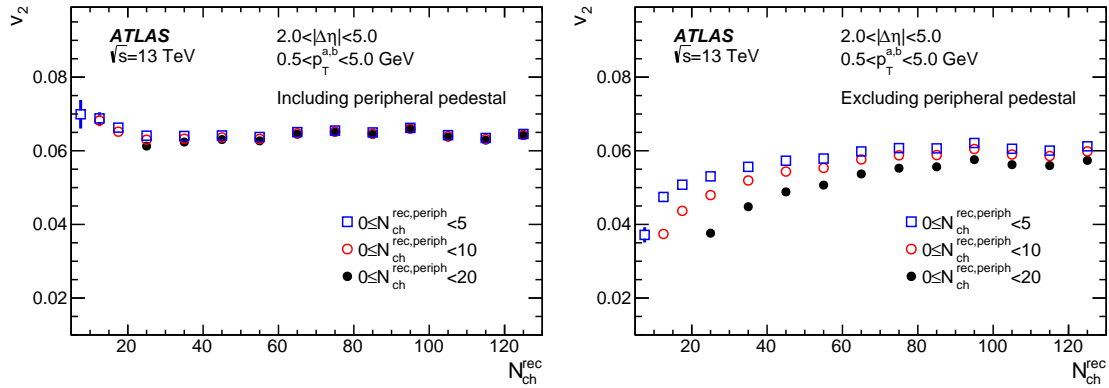


Fig. 3. The multiplicity dependence v_2 for $0.5 < p_T < 5.0$ GeV/c for three different low-multiplicity samples in pp collisions at 13 TeV using the ATLAS template fit method allowing for non-zero v_2 in the low multiplicity sample (left panel) or assuming it to be zero (right panel), in which case the template fit is equivalent to the subtraction method. Minimum bias collisions roughly correspond to $N_{ch}^{rec} \approx 15$. Auxiliary figure 13 from Ref. [65].

shape of low multiplicity event class.¹⁴ Hence, it may be useful to repeat the analysis with a lower p_T cut of at least $p_T > 0.7$ GeV/c, for which near- and away-side associated yields have a similar slope with multiplicity [164]. In the case of CMS, contributions from lowest multiplicity are reduced, because events with less than 10 tracks are excluded from the low multiplicity sample, however, a lower p_T cut of 0.3 instead of 0.5 GeV/c is used. Though, as mentioned in Sec. 3, one usually ensures that the low-multiplicity sample used in the subtraction procedure does not reveal unknown features (for example in the case of pPb by comparing with minimum bias pp [26]). Since changing the range of the low multiplicity sample changes the measured v_2 , one can attempt to correct the measured v_2 for an assumed fraction of v_2^0 present in the low multiplicity sample. To achieve this a template fit of the scaled low multiplicity yield with an added $G(1 + 2V_2 \cos(2\Delta\phi))$ term is used by ATLAS to extract $\frac{GV_2 - FG_0 v_2^0}{G - FG_0}$, thus measuring approximately V_2 if $V_2^0 \approx V_2$ ¹⁵ (G_0 is the baseline in the low-multiplicity class) [65]. In this case, the measured v_2 values are found to be rather constant with multiplicity for $M \gtrsim 20$, essentially the same for different choices of constructing the low multiplicity sample, and about 10% larger than the results from the subtraction method at high M (see left panel of Fig. 3). Below $M < 20$ the v_2 values slightly increase with decreasing M indicating that there are indeed larger modifications to the long-range correlation structures present in such low multiplicity events, perhaps related to diffraction and hadronization, as discussed above. The consistency of the results support the assumption of a constant v_2 , which can not be proven for the lower multiplicity events, but holds already for $M > 20$. Instead, if one assumes that $v_2 = 0$ for $M < 20$, then the measured v_2 values increase with multiplicity, reaching asymptotically similar values as for the constant v_2 case, because the assumption about v_2 in the low multiplicity event has ever decreasing influence. Above $M \gtrsim 70$, the two methods lead to v_2 values with differences within about 20%, representing a robust measurement of v_2 at high multiplicity. At lower M , the spread of the v_2 values indicates that more studies are needed, but independent of the assumption even in events with $M > 30$ (roughly twice of minimum bias collisions) a significant value of $v_2 \approx 0.04$ is obtained. Measurements involving four- and six-particle cumulants [67], which earlier did not reach conclusive results [66, 119], reveal that $v_2\{4\} \approx v_2\{6\} > 0$ even in pp collisions at high multiplicity ($M > 75$) consistent with the emergence of collective behavior. However, these measurements, in particular for small

¹⁴It is important to define the correlation function as a “ratio of sums” and not as a “sum of ratios”, as briefly mentioned in [26], in order to avoid inherent multiplicity-dependent effects in the measurement of the correlation function.

¹⁵This way to extract V_2 is called “Including peripheral pedestal” by ATLAS to indicate that the resulting V_2 from the template fit is not further corrected by the baseline of the higher multiplicity event class. This is different from the case, which is labeled “Excluding peripheral pedestal”, where the V_2 returned by the fit is divided by the baseline of the higher multiplicity class, as explained for the subtraction method above.

M , need sufficiently high statistics and can not resolve the conceptual difference between including and excluding the pedestal in the subtraction discussed above. Already now results of v_2 versus p_T for K_S^0 and Λ have been presented [67] and for high multiplicity reveal a similar characteristic mass dependence as in pPb and PbPb collisions, which is absent in low multiplicity events, and may be interpreted as strong support for a hydrodynamic behavior [165]. The shape and even the magnitude of the long-range component of two particle-pseudorapidity correlations are found to be similar for pp, pPb and PbPb at similar multiplicity [90], which may be used to constrain calculations of the initial state for the three systems. Other effects, in particular related to jet quenching[166], are not straightforward to measure because of difficulties to define a rigorous normalization for nuclear effects, which is already a challenge in the case of pPb due to the contribution from multiple-parton interactions [121]. In pp even more than in pPb collisions there is a complex interplay between hard, multiple semi-hard and soft processes [113, 164, 167–171], which needs to be disentangled from nuclear modification.

5. Discussion and concluding remarks

The previous sections briefly described measurements, and their common interpretation, in PbPb, as well as in high multiplicity pPb and pp collisions, following the summary given in Table 1. Weak collectivity (i.e. the agreement of higher-order cumulant and LYZ methods) is established within the experimental uncertainties in PbPb and pPb collisions, and starts to emerge even in pp collisions ($v_2\{4\} \approx v_2\{6\}$). However, it should also be seen in e^+e^- collisions (see Fig. 2). Most observables in PbPb and high multiplicity pPb collisions can even be explained assuming strong collectivity, i.e. as a system described by thermo- and hydrodynamics. There is less information available at high multiplicity for pp collisions, however—where available—the trends are similar as for pPb (for a recent review on these topics, see Ref. [172]). Naturally, similar observations could be caused by similar or even common physics. Assuming that the underlying physics is the same for the observed phenomena, what are the possible common explanations?

i) A natural candidate for a system exhibiting strong collective effects is of course the sQGP [173], which appears to flow almost like a perfect fluid with its shear-viscosity to entropy-density ratio η/s close to the theoretical lower bound [174]. In pPb and even more in pp collisions, one expects a stronger radial flow¹⁶ than in PbPb at similar multiplicities, because an approximately scale-invariant system would be smaller but hotter, leading to longer cooling and expansion [138, 175]. As for PbPb, hydrodynamic calculations quantitatively describe the small-system data [177], and even the magnitude of v_2 in pp has been successfully predicted [178, 179]. In case of the proton, however, sub-nuclear scales in modelling the initial state become important and, since they are not well known, result in a larger ambiguity of the calculations [180]. A challenge for the sQGP picture is the presence of a finite v_2 at 10 GeV/c (even though with large uncertainties) [64] without direct evidence of jet quenching in the charged-particle Q_{pPb} [121], while jet calculations indicate a significant, but with the present uncertainties difficult to measure, jet quenching effect [154]. In the low density limit, v_2 is expected to scale with multiplicity (as a proxy for the density of the system), while v_2 should saturate in the hydrodynamic limit [181]. Taking the v_2 results from ATLAS in pp collisions at face value [65], one would have hydrodynamically generated v_2 down to very low multiplicity, i.e. sQGP droplets form in essentially every (non-diffractive) pp event at 13 TeV, which seems quite surprising.¹⁷ However, significant progress has been achieved in the past, by pushing the picture of the almost perfect fluid ever further, following “naturalness” arguments, exemplified in the following: The large v_2 in central CuCu collisions at $\sqrt{s_{NN}} = 200$ GeV, which was found to be indeed larger than in AuAu collisions and hence larger than expected from hydrodynamics, was explained by postulating the relevance of eccentricity fluctuations, and in particular the “participant eccentricity” [183]. The participant eccentricity, which predicted characteristic flow fluctuations consistent with a later measurement [184], was generalized

¹⁶Originally, radial flow was suggested to be present in pp collision even at ISR collision energies [176].

¹⁷However, the formation of a deconfined system in such collisions can not apriori be excluded. The charged-particle mid-rapidity density at 13 TeV for events with one track (INEL>0) is 6.46 ± 0.19 [182], which would lead to an energy density above 1.5 GeV/fm^3 for $\tau < 1 \text{ fm/c}$ assuming an average p_T as measured for 7 TeV pp collisions[158].

to “triangularity” and highlighted the relevance of higher moments in the initial state [185]. The triangular structures only became directly visible in the PbPb data [60, 76], and today the pPb and pp data could not have been understood in the hydrodynamic picture without acknowledging the relevance of initial state fluctuations. Further, prompted by the similarity of v_3 in pPb and PbPb [29], the hydrodynamic paradigm was successfully tested in $^3\text{HeAu}$ collisions at RHIC [186], where the use of Helium-3 was expected to enhance the observed v_3 due to the intrinsic triangular shape of its wavefunction [187]. Nevertheless, despite its success, it must be emphasized that hydrodynamics can not explain how the system is brought into (approximate) equilibrium, and its use by construction hides any underlying microscopic physics picture.

ii) A second possibility is to explain the observed phenomena with parton transport models, such as BAMPS [188] or AMPT [189], which employ non-equilibrium parton dynamics. These calculations attempt to microscopically describe the underlying physics, and may be able to lead from weak to strong collectivity depending on the parton density and interaction cross sections. Indeed, early calculations were argued to support the effective use of ideal hydrodynamics because one needed to inflate the (elastic) partonic cross sections (σ) from about 3 to 45 mb (i.e. to hadronic level) for a realistic initial gluon density of 1000–1500 at mid-rapidity, in order to explain the early v_2 results in AuAu collisions at $\sqrt{s_{NN}} = 130$ [190]. Today we know that AMPT with much lower cross sections of 1.5 to 3 mb can reproduce most of the experimental findings [191–194]. AMPT, which was used to substantiate the postulation of triangularity [185], had even incorporated the underlying initial-state fluctuations and their influence on final azimuthal particle spectra before they were identified to be relevant. However, in AMPT the azimuthal anisotropies are produced mainly by the anisotropic parton escape probability as a response to the initial spatial eccentricity with no or only a few parton interactions, not necessarily by pressure-driven collective flow.¹⁸ The contribution to the final v_2 from the escape probability is also found to be significant (about 30–40% even for $\sigma = 45$ mb) in semi-central (about 20%) nucleus–nucleus collisions [195, 196]. Additionally, AMPT generates the characteristic dependence of v_2 on the particle mass from kinematics in the implemented coalescence approach and hadronic rescatterings [197]. These recent conclusions drawn from studies using AMPT question aspects of the perfect liquid paradigm, perhaps even in semi-central and central AA collisions. However, despite the fact that AMPT describes a wealth of the data, it is important to realize that the above conclusions depend on an interplay of questionable and not yet fully understood concepts such as string melting (resulting in the presence of a large number of quark/antiquark pairs and zero gluons), p_T dependent parton formation and spatial coalescence. Hence, follow-up studies, in particular on the relevance of the escape mechanism, using a different transport model, such as BAMPS, and viscous hydrodynamic calculations are needed. Recently, it also was reported that non-hydrodynamic (free streaming) evolution can generally create equal or larger radial flow than hydrodynamics (with $\eta/s = 0.08$) [198, 199]. In pPb collisions free streaming leads to large v_3 , but considerably smaller v_2 than from hydrodynamics, while as expected it cannot account for the observed harmonics in PbPb collisions. Since pre-equilibrium dynamics and hadronic interactions are expected to play a significant role in small systems, a beam energy scan of dAu collisions at RHIC may shed light on the question of whether equilibrium dynamics is indeed the source of the observed collectivity [200].

iii) The third possibility could be correlations present in the initial state followed by a suitable “evolution”, perhaps leading from Yang-Mills evolution in smaller systems to hydrodynamic evolution in larger systems. The glasma graph framework derived in the context of the Color Glas Condensate (CGC) is able to describe many features of two-particle correlations [33, 201, 202], including the long range nature, the double ridge structure, the strength and shape, the non-trivial multiplicity dependence, as well as mass ordering of mean p_T and v_2 in pp and pPb collisions. However, the original calculation can neither account for genuine multi-particle correlations, nor for the presence of odd harmonics, most notably v_3 . Explaining these data has been achieved by using classical Yang-Mills simulations on the lattice [155, 203], which incorporate contributions from glasma graphs, from perturbatively disconnected graphs (which connect through

¹⁸A finite contribution to v_2 from an azimuthally non-uniform escape probability is expected to be generated in a pre-equilibrium phase, because only colliding particles contribute to the eventual formation of approximate equilibrium, while those with no or few collisions leave the collision zone, contributing to escape v_2 . It is an open question to what extent viscous hydrodynamic calculations include the effect, and whether it indeed is conceptually different from collective flow, or not a necessary ingredient. However, v_2 from escape does not require a hydrodynamic phase.

event-by-event breaking of rotational symmetry into domains with a size related to the inverse of the saturation scale [204, 205]), as well as from final state interactions generated by the Yang-Mills evolution. In these simulations, the gluons already have a large v_2 in the initial state, albeit a v_3 of zero. However, after the time $\tau \leq 0.4$ fm/c final state effects induced by the classical Yang-Mills evolution generate a non-zero v_3 with only little modification of v_2 . In contrast, Yang-Mills simulations of PbPb collisions exhibit much smaller values of v_2 and v_3 , since the contribution from disconnected graphs is significantly reduced due to the increase in the number of uncorrelated domains. Therefore, additional collective flow effects are needed to explain the PbPb data. However, so far these Yang-Mills simulations neglect contribution from jet graphs (which at higher order may become relevant) and effects from hadronization, which are also considered to be important [206]. Furthermore, the forward and backward v_2 results in pPb [88] question ideas based on the CGC, because the saturation scale dependence on rapidity would predict v_2 on the Pb side to be smaller than on the proton side, while the data indicate an opposite trend, qualitatively consistent with expectations from hydrodynamics and AMPT [207, 208]. In general, there is not yet a single framework that can quantitatively describe all data on similar footing, but effort in this direction is ongoing [209]. In conclusion, the study of small systems may allow us to probe dynamics rather than equilibrium (with a further handle on possible viscous effects), to potentially validate or invalidate the “perfect fluidity” paradigm, and to test fundamental QCD due to relevance of sub-nucleon degrees of freedom in the initial state.

Acknowledgments

I would like to thank the organizers for creating an interesting and stimulating conference. Fruitful discussions with J. Schukraft are acknowledged. Special thanks to M. Fasel, J. Kamin and L. Milano for critical reading of the draft. This work is supported in part by the U.S. Department of Energy, Office of Science, Office of Nuclear Physics, under contract number DE-AC02-05CH11231.

References

- [1] U. A. Wiedemann, Jet quenching in heavy ion collisions (2010) 521–562 [Landolt-Bornstein23,521(2010)]. [arXiv:0908.2306](#).
- [2] S. A. Voloshin, A. M. Poskanzer, R. Snellings, Collective phenomena in non-central nuclear collisions [arXiv:0809.2949](#).
- [3] M. Gyulassy, The QGP discovered at RHIC (2004) 159–182 [arXiv:nuc1-th/0403032](#).
- [4] C. Salgado, J. Alvarez-Muniz, F. Arleo, N. Armesto, M. Botje, et al., Proton–nucleus collisions at the LHC: Scientific opportunities and requirements, *J.Phys. G*39 (2012) 015010. [arXiv:1105.3919](#), [doi:10.1088/0954-3889/39/1/015010](#).
- [5] B. B. Back, et al., Centrality dependence of charged hadron transverse momentum spectra in dAu collisions at $\sqrt{s_{NN}} = 200$ GeV, *Phys. Rev. Lett.* 91 (2003) 072302. [arXiv:nuc1-ex/0306025](#), [doi:10.1103/PhysRevLett.91.072302](#).
- [6] S. S. Adler, et al., Absence of suppression in particle production at large transverse momentum in $\sqrt{s_{NN}} = 200$ GeV dAu collisions, *Phys. Rev. Lett.* 91 (2003) 072303. [arXiv:nuc1-ex/0306021](#), [doi:10.1103/PhysRevLett.91.072303](#).
- [7] J. Adams, et al., Evidence from dAu measurements for final state suppression of high p_T hadrons in AuAu collisions at RHIC, *Phys. Rev. Lett.* 91 (2003) 072304. [arXiv:nuc1-ex/0306024](#), [doi:10.1103/PhysRevLett.91.072304](#).
- [8] I. Arsene, et al., Transverse momentum spectra in AuAu and dAu collisions at $\sqrt{s_{NN}} = 200$ GeV and the pseudorapidity dependence of high- p_T suppression, *Phys. Rev. Lett.* 91 (2003) 072305. [arXiv:nuc1-ex/0307003](#), [doi:10.1103/PhysRevLett.91.072305](#).
- [9] B. Abelev, et al., Transverse momentum distribution and nuclear modification factor of charged particles in pPb collisions at $\sqrt{s_{NN}} = 5.02$ TeV, *Phys. Rev. Lett.* 110 (8) (2013) 082302. [arXiv:1210.4520](#), [doi:10.1103/PhysRevLett.110.082302](#).
- [10] B. Abelev, et al., Transverse momentum dependence of inclusive primary charged-particle production in pPb collisions at $\sqrt{s_{NN}} = 5.02$ TeV, *Eur. Phys. J. C*74 (9) (2014) 3054. [arXiv:1405.2737](#), [doi:10.1140/epjc/s10052-014-3054-5](#).
- [11] V. Khachatryan, et al., Nuclear effects on the transverse momentum spectra of charged particles in pPb collisions at $\sqrt{s_{NN}} = 5.02$ TeV, *Eur. Phys. J. C*75 (5) (2015) 237. [arXiv:1502.05387](#), [doi:10.1140/epjc/s10052-015-3435-4](#).
- [12] J. Adam, et al., Measurement of charged jet production cross sections and nuclear modification in pPb collisions at $\sqrt{s_{NN}} = 5.02$ TeV, *Phys. Lett. B*749 (2015) 68–81. [arXiv:1503.00681](#), [doi:10.1016/j.physletb.2015.07.054](#).
- [13] V. Khachatryan, et al., Measurement of inclusive jet production and nuclear modifications in pPb collisions at $\sqrt{s_{NN}} = 5.02$ TeV [arXiv:1601.02001](#).
- [14] B. Abelev, et al., J/ψ production and nuclear effects in pPb collisions at $\sqrt{s_{NN}} = 5.02$ TeV, *JHEP* 02 (2014) 073. [arXiv:1308.6726](#), [doi:10.1007/JHEP02\(2014\)073](#).
- [15] R. Aaij, et al., Study of J/ψ production and cold nuclear matter effects in pPb collisions at $\sqrt{s_{NN}} = 5$ TeV, *JHEP* 02 (2014) 072. [arXiv:1308.6729](#), [doi:10.1007/JHEP02\(2014\)072](#).
- [16] J. Adam, et al., Rapidity and transverse-momentum dependence of the inclusive J/ψ nuclear modification factor in pPb collisions at $\sqrt{s_{NN}} = 5.02$ TeV, *JHEP* 06 (2015) 055. [arXiv:1503.07179](#), [doi:10.1007/JHEP06\(2015\)055](#).

- [17] G. Aad, et al., Measurement of differential J/ψ production cross sections and forward-backward ratios in pPb collisions with the ATLAS detector, *Phys. Rev. C* 92 (3) (2015) 034904. [arXiv:1505.08141](#), [doi:10.1103/PhysRevC.92.034904](#).
- [18] B. Abelev, et al., Measurement of prompt D -meson production in pPb collisions at $\sqrt{s_{NN}} = 5.02$ TeV, *Phys. Rev. Lett.* 113 (23) (2014) 232301. [arXiv:1405.3452](#), [doi:10.1103/PhysRevLett.113.232301](#).
- [19] B. Abelev, et al., Production of inclusive $\Upsilon(1S)$ and $\Upsilon(2S)$ in pPb collisions at $\sqrt{s_{NN}} = 5.02$ TeV, *Phys. Lett. B* 740 (2015) 105–117. [arXiv:1410.2234](#), [doi:10.1016/j.physletb.2014.11.041](#).
- [20] R. Aaij, et al., Study of Υ production and cold nuclear matter effects in pPb collisions at $\sqrt{s_{NN}} = 5$ TeV, *JHEP* 07 (2014) 094. [arXiv:1405.5152](#), [doi:10.1007/JHEP07\(2014\)094](#).
- [21] V. Khachatryan, et al., Study of B meson production in pPb collisions at $\sqrt{s_{NN}} = 5.02$ TeV, *Phys. Rev. Lett.* 116 (3) (2016) 032301. [arXiv:1508.06678](#), [doi:10.1103/PhysRevLett.116.032301](#).
- [22] V. Khachatryan, et al., Transverse momentum spectra of inclusive b jets in pPb collisions at $\sqrt{s_{NN}} = 5.02$ TeV, *Phys. Lett. B* 754 (2016) 59–80. [arXiv:1510.03373](#), [doi:10.1016/j.physletb.2016.01.010](#).
- [23] J. Adam, et al., Measurement of electrons from heavy-flavour hadron decays in pPb collisions at $\sqrt{s_{NN}} = 5.02$ TeV, [arXiv:1509.07491](#).
- [24] S. Chatrchyan, et al., Evidence of b-jet quenching in PbPb collisions at $\sqrt{s_{NN}} = 2.76$ TeV, *Phys. Rev. Lett.* 113 (13) (2014) 132301. [arXiv:1312.4198](#), [doi:10.1103/PhysRevLett.113.132301](#).
- [25] S. Chatrchyan, et al., Observation of long-range near-side angular correlations in pPb collisions at the LHC, *Phys. Lett. B* 718 (2013) 795–814. [arXiv:1210.5482](#), [doi:10.1016/j.physletb.2012.11.025](#).
- [26] B. Abelev, et al., Long-range angular correlations on the near and away side in pPb collisions at $\sqrt{s_{NN}} = 5.02$ TeV, *Phys. Lett. B* 719 (2013) 29–41. [arXiv:1212.2001](#), [doi:10.1016/j.physletb.2013.01.012](#).
- [27] G. Aad, et al., Observation of associated near-side and away-side long-range correlations in $\sqrt{s_{NN}} = 5.02$ TeV pPb collisions with the ATLAS detector, *Phys. Rev. Lett.* 110 (18) (2013) 182302. [arXiv:1212.5198](#), [doi:10.1103/PhysRevLett.110.182302](#).
- [28] G. Aad, et al., Measurement with the ATLAS detector of multi-particle azimuthal correlations in pPb collisions at $\sqrt{s_{NN}} = 5.02$ TeV, *Phys. Lett. B* 725 (2013) 60–78. [arXiv:1303.2084](#), [doi:10.1016/j.physletb.2013.06.057](#).
- [29] S. Chatrchyan, et al., Multiplicity and transverse momentum dependence of two- and four-particle correlations in pPb and PbPb collisions, *Phys. Lett. B* 724 (2013) 213–240. [arXiv:1305.0609](#), [doi:10.1016/j.physletb.2013.06.028](#).
- [30] C. Loizides, First results from pPb collisions at the LHC, *EPJ Web Conf.* 60 (2013) 06004. [arXiv:1308.1377](#), [doi:10.1051/epjconf/20136006004](#).
- [31] V. Khachatryan, et al., Observation of long-range near-side angular correlations in pp collisions at the LHC, *JHEP* 09 (2010) 091. [arXiv:1009.4122](#), [doi:10.1007/JHEP09\(2010\)091](#).
- [32] P. Bozek, W. Broniowski, Collective dynamics in high-energy proton-nucleus collisions, *Phys. Rev. C* 88 (1) (2013) 014903. [arXiv:1304.3044](#), [doi:10.1103/PhysRevC.88.014903](#).
- [33] K. Dusling, R. Venugopalan, Comparison of the color glass condensate to dihadron correlations in proton-proton and proton-nucleus collisions, *Phys. Rev. D* 87 (9) (2013) 094034. [arXiv:1302.7018](#), [doi:10.1103/PhysRevD.87.094034](#).
- [34] C. Loizides, Experimental overview on small colliding systems at LHC, <http://indico.cern.ch/event/355454/session/0/contribution/102>.
- [35] J. Adams, et al., Azimuthal anisotropy in AuAu collisions at $\sqrt{s_{NN}} = 200$ GeV, *Phys. Rev. C* 72 (2005) 014904. [arXiv:nucl-ex/0409033](#), [doi:10.1103/PhysRevC.72.014904](#).
- [36] P. Stankus, Experimental overview on small colliding systems at RHIC, *Nucl. Phys. A* (2016) these proceedings.
- [37] B. Abelev, et al., Pion, kaon, and proton production in central PbPb collisions at $\sqrt{s_{NN}} = 2.76$ TeV, *Phys. Rev. Lett.* 109 (2012) 252301. [arXiv:1208.1974](#), [doi:10.1103/PhysRevLett.109.252301](#).
- [38] B. Abelev, et al., Centrality dependence of π , K, p production in PbPb collisions at $\sqrt{s_{NN}} = 2.76$ TeV, *Phys. Rev. C* 88 (2013) 044910. [arXiv:1303.0737](#), [doi:10.1103/PhysRevC.88.044910](#).
- [39] S. Chatrchyan, et al., Study of the production of charged pions, kaons, and protons in pPb collisions at $\sqrt{s_{NN}} = 5.02$ TeV, *Eur. Phys. J. C* 74 (6) (2014) 2847. [arXiv:1307.3442](#), [doi:10.1140/epjc/s10052-014-2847-x](#).
- [40] S. Chatrchyan, et al., Study of the inclusive production of charged pions, kaons, and protons in pp collisions at $\sqrt{s} = 0.9, 2.76$, and 7 TeV, *Eur. Phys. J. C* 72 (2012) 2164. [arXiv:1207.4724](#), [doi:10.1140/epjc/s10052-012-2164-1](#).
- [41] C. Andrei (for the ALICE collaboration), Light flavor hadron spectra at low p_T and search for collective phenomena in high multiplicity pp, pPb and PbPb collisions measured with the ALICE experiment, *Nucl. Phys. A* 931 (2014) 888–892. [arXiv:1408.0093](#), [doi:10.1016/j.nuclphysa.2014.08.002](#).
- [42] B. Abelev, et al., Multiplicity dependence of pion, kaon, proton and Λ production in pPb collisions at $\sqrt{s_{NN}} = 5.02$ TeV, *Phys. Lett. B* 728 (2014) 25–38. [arXiv:1307.6796](#), [doi:10.1016/j.physletb.2013.11.020](#).
- [43] B. Abelev, et al., K_S^0 and Λ production in PbPb collisions at $\sqrt{s_{NN}} = 2.76$ TeV, *Phys. Rev. Lett.* 111 (2013) 222301. [arXiv:1307.5530](#), [doi:10.1103/PhysRevLett.111.222301](#).
- [44] B. Abelev, et al., $K^*(892)^0$ and $\phi(1020)$ production in PbPb collisions at $\sqrt{s_{NN}} = 2.76$ TeV, *Phys. Rev. C* 91 (2015) 024609. [arXiv:1404.0495](#), [doi:10.1103/PhysRevC.91.024609](#).
- [45] V. Khachatryan, et al., Multiplicity and rapidity dependence of strange hadron production in pp, pPb and PbPb collisions at the LHC, Submitted to: *Phys. Lett. B* [arXiv:1605.06699](#).
- [46] J. Adam, et al., ϕ -meson production at forward rapidity in pPb collisions at $\sqrt{s_{NN}} = 5.02$ TeV and in pp collisions at $\sqrt{s} = 2.76$ TeV, [arXiv:1506.09206](#).
- [47] J. Adam, et al., Multiplicity dependence of charged pion, kaon, and (anti)proton production at large transverse momentum in pPb collisions at $\sqrt{s_{NN}} = 5.02$ TeV, [arXiv:1601.03658](#).
- [48] J. Adam, et al., Multiplicity-dependent enhancement of strange and multi-strange hadron production in proton-proton collisions at $\sqrt{s} = 7$ TeV, [arXiv:1606.07424](#).
- [49] J. Adam, et al., Production of $K^*(892)^0$ and $\phi(1020)$ in pPb collisions at $\sqrt{s_{NN}} = 5.02$ TeV, [arXiv:1601.07868](#).

- [50] J. Adam, et al., Multi-strange baryon production in pPb collisions at $\sqrt{s_{NN}} = 5.02$ TeV [arXiv:1512.07227](#).
- [51] B. B. Abelev, et al., Multi-strange baryon production at mid-rapidity in PbPb collisions at $\sqrt{s_{NN}} = 2.76$ TeV, *Phys. Lett. B* 728 (2014) 216–227. [arXiv:1307.5543](#), doi:10.1016/j.physletb.2014.05.052, 10.1016/j.physletb.2013.11.048.
- [52] M. Floris, Hadron yields and the phase diagram of strongly interacting matter, *Nucl. Phys. A* 931 (2014) 103–112. [arXiv:1408.6403](#), doi:10.1016/j.nuclphysa.2014.09.002.
- [53] J. Adam, et al., Centrality dependence of pion freeze-out radii in PbPb collisions at $\sqrt{s_{NN}} = 2.76$ TeV [arXiv:1507.06842](#).
- [54] J. Adam, et al., One-dimensional pion, kaon, and proton femtoscopy in PbPb collisions at $\sqrt{s_{NN}} = 2.76$ TeV, *Phys. Rev. C* 92 (2015) 054908. [arXiv:1506.07884](#), doi:10.1103/PhysRevC.92.054908.
- [55] B. Abelev, et al., Freeze-out radii extracted from three-pion cumulants in pp, pPb and PbPb collisions at the LHC, *Phys. Lett. B* 739 (2014) 139–151. [arXiv:1404.1194](#), doi:10.1016/j.physletb.2014.10.034.
- [56] J. Adam, et al., Two-pion femtoscopy in pPb collisions at $\sqrt{s_{NN}} = 5.02$ TeV, *Phys. Rev. C* 91 (2015) 034906. [arXiv:1502.00559](#), doi:10.1103/PhysRevC.91.034906.
- [57] K. Aamodt, et al., Femtoscopy of pp collisions at $\sqrt{s} = 0.9$ and 7 TeV at the LHC with two-pion Bose-Einstein correlations, *Phys. Rev. D* 84 (2011) 112004. [arXiv:1101.3665](#), doi:10.1103/PhysRevD.84.112004.
- [58] V. Khachatryan, et al., Femtoscopy with identified charged hadrons in pp, pPb, and peripheral PbPb collisions at LHC energies, CMS-PAS-HIN-14-013.
- [59] A. G., et al., Femtoscopy with identified charged pions in proton-lead collisions at $\sqrt{s_{NN}} = 5.02$ TeV with ATLAS, ATLAS-CONF-2015-054.
- [60] K. Aamodt, et al., Harmonic decomposition of two-particle angular correlations in PbPb collisions at $\sqrt{s_{NN}} = 2.76$ TeV, *Phys. Lett. B* 708 (2012) 249–264. [arXiv:1109.2501](#), doi:10.1016/j.physletb.2012.01.060.
- [61] S. Chatrchyan, et al., Long-range and short-range dihadron angular correlations in central PbPb collisions at a nucleon-nucleon center of mass energy of 2.76 TeV, *JHEP* 07 (2011) 076. [arXiv:1105.2438](#), doi:10.1007/JHEP07(2011)076.
- [62] S. Chatrchyan, et al., Centrality dependence of dihadron correlations and azimuthal anisotropy harmonics in PbPb collisions at $\sqrt{s_{NN}} = 2.76$ TeV, *Eur. Phys. J. C* 72 (2012) 2012. [arXiv:1201.3158](#), doi:10.1140/epjc/s10052-012-2012-3.
- [63] G. Aad, et al., Measurement of the azimuthal anisotropy for charged particle production in $\sqrt{s_{NN}} = 2.76$ TeV lead-lead collisions with the ATLAS detector, *Phys. Rev. C* 86 (2012) 014907. [arXiv:1203.3087](#), doi:10.1103/PhysRevC.86.014907.
- [64] G. Aad, et al., Measurement of long-range pseudorapidity correlations and azimuthal harmonics in $\sqrt{s_{NN}} = 5.02$ TeV proton-lead collisions with the ATLAS detector, *Phys. Rev. C* 90 (4) (2014) 044906. [arXiv:1409.1792](#), doi:10.1103/PhysRevC.90.044906.
- [65] G. Aad, et al., Observation of long-range elliptic anisotropies in $\sqrt{s} = 13$ and 2.76 TeV pp collisions with the ATLAS detector [arXiv:1509.04776](#).
- [66] V. Khachatryan, et al., Observation of long-range near-side two-particle correlations in pp collisions at $\sqrt{s} = 13$ TeV, CMS-PAS-FSQ-15-002.
- [67] V. Khachatryan, et al., Evidence for collectivity in pp collisions at the LHC, Submitted to: Physics Letters [arXiv:1606.06198](#).
- [68] B. Abelev, et al., Elliptic flow of identified hadrons in PbPb collisions at $\sqrt{s_{NN}} = 2.76$ TeV, *JHEP* 06 (2015) 190. [arXiv:1405.4632](#), doi:10.1007/JHEP06(2015)190.
- [69] B. Abelev, et al., Anisotropic flow of charged hadrons, pions and (anti-)protons measured at high transverse momentum in PbPb collisions at $\sqrt{s_{NN}} = 2.76$ TeV, *Phys. Lett. B* 719 (2013) 18–28. [arXiv:1205.5761](#), doi:10.1016/j.physletb.2012.12.066.
- [70] J. Adam, et al., Higher harmonic flow coefficients of identified hadrons in PbPb collisions at $\sqrt{s_{NN}} = 2.76$ TeV [arXiv:1606.06057](#).
- [71] V. Khachatryan, et al., Long-range two-particle correlations of strange hadrons with charged particles in pPb and PbPb collisions at LHC energies, *Phys. Lett. B* 742 (2015) 200–224. [arXiv:1409.3392](#), doi:10.1016/j.physletb.2015.01.034.
- [72] B. Abelev, et al., Long-range angular correlations of π , K and p in pPb collisions at $\sqrt{s_{NN}} = 5.02$ TeV, *Phys. Lett. B* 726 (2013) 164–177. [arXiv:1307.3237](#), doi:10.1016/j.physletb.2013.08.024.
- [73] V. Khachatryan, et al., Azimuthal anisotropy harmonics from long-range correlations in high multiplicity pp collisions at $\sqrt{s} = 7$ TeV, CMS-PAS-HIN-15-009.
- [74] B. Abelev, et al., Directed flow of charged particles at midrapidity relative to the spectator plane in PbPb collisions at $\sqrt{s_{NN}} = 2.76$ TeV, *Phys. Rev. Lett.* 111 (23) (2013) 232302. [arXiv:1306.4145](#), doi:10.1103/PhysRevLett.111.232302.
- [75] K. Aamodt, et al., Elliptic flow of charged particles in PbPb collisions at 2.76 TeV, *Phys. Rev. Lett.* 105 (2010) 252302. [arXiv:1011.3914](#), doi:10.1103/PhysRevLett.105.252302.
- [76] K. Aamodt, et al., Higher harmonic anisotropic flow measurements of charged particles in PbPb collisions at $\sqrt{s_{NN}} = 2.76$ TeV, *Phys. Rev. Lett.* 107 (2011) 032301. [arXiv:1105.3865](#), doi:10.1103/PhysRevLett.107.032301.
- [77] S. Chatrchyan, et al., Measurement of the elliptic anisotropy of charged particles produced in PbPb collisions at $\sqrt{s_{NN}} = 2.76$ TeV, *Phys. Rev. C* 87 (1) (2013) 014902. [arXiv:1204.1409](#), doi:10.1103/PhysRevC.87.014902.
- [78] B. Abelev, et al., Multiparticle azimuthal correlations in pPb and PbPb collisions at the CERN Large Hadron Collider, *Phys. Rev. C* 90 (5) (2014) 054901. [arXiv:1406.2474](#), doi:10.1103/PhysRevC.90.054901.
- [79] S. Chatrchyan, et al., Measurement of higher-order harmonic azimuthal anisotropy in PbPb collisions at $\sqrt{s_{NN}} = 2.76$ TeV, *Phys. Rev. C* 89 (4) (2014) 044906. [arXiv:1310.8651](#), doi:10.1103/PhysRevC.89.044906.
- [80] G. Aad, et al., Measurement of flow harmonics with multi-particle cumulants in PbPb collisions at $\sqrt{s_{NN}} = 2.76$ TeV with the ATLAS detector, *Eur. Phys. J. C* 74 (11) (2014) 3157. [arXiv:1408.4342](#), doi:10.1140/epjc/s10052-014-3157-z.
- [81] V. Khachatryan, et al., Evidence for collective multiparticle correlations in pPb collisions, *Phys. Rev. Lett.* 115 (1) (2015) 012301. [arXiv:1502.05382](#), doi:10.1103/PhysRevLett.115.012301.
- [82] J. Adam, et al., Anisotropic flow of charged particles in PbPb collisions at $\sqrt{s_{NN}} = 5.02$ TeV [arXiv:1602.01119](#).

- [83] V. Khachatryan, et al., Differential flow harmonic v_n in pPb and PbPb collisions, CMS-PAS-HIN-15-008.
- [84] J. Adam, et al., Pseudorapidity dependence of the anisotropic flow of charged particles in PbPb collisions at $\sqrt{s_{NN}} = 2.76$ TeV, *Phys. Lett. B* 753 (2016) 126–139. [arXiv:1605.02035](#), [doi:10.1016/j.physletb.2016.07.017](#).
- [85] G. Aad, et al., Measurement of the centrality and pseudorapidity dependence of the integrated elliptic flow in lead-lead collisions at $\sqrt{s_{NN}} = 2.76$ TeV with the ATLAS detector, *Eur. Phys. J. C* 74 (8) (2014) 2982. [arXiv:1405.3936](#), [doi:10.1140/epjc/s10052-014-2982-4](#).
- [86] G. Aad, et al., Measurement of the pseudorapidity and transverse momentum dependence of the elliptic flow of charged particles in lead-lead collisions at $\sqrt{s_{NN}} = 2.76$ TeV with the ATLAS detector, *Phys. Lett. B* 707 (2012) 330–348. [arXiv:1108.6018](#), [doi:10.1016/j.physletb.2011.12.056](#).
- [87] V. Khachatryan, et al., Pseudorapidity dependence of long-range two-particle correlations in pPb collisions at $\sqrt{s_{NN}} = 5.02$ TeV, *Phys. Lett. B* 753 (2016) 126–139. [arXiv:1506.08032](#), [doi:10.1016/j.physletb.2015.12.010](#).
- [88] J. Adam, et al., Forward-central two-particle correlations in pPb collisions at $\sqrt{s_{NN}} = 5.02$ TeV, *Phys. Lett. B* 753 (2016) 126–139. [arXiv:1506.08032](#), [doi:10.1016/j.physletb.2015.12.010](#).
- [89] R. Aaij, et al., Measurements of long-range near-side angular correlations in $\sqrt{s_{NN}} = 5$ TeV proton-lead collisions in the forward region, *Phys. Lett. B* 753 (2016) 126–139. [arXiv:1512.00439](#).
- [90] M. Aaboud, et al., Measurement of forward-backward multiplicity correlations in lead-lead, proton-lead and proton-proton collisions with the ATLAS detector, *Phys. Lett. B* 753 (2016) 126–139. [arXiv:1606.08170](#).
- [91] V. Khachatryan, et al., Evidence for transverse momentum and pseudorapidity dependent event plane fluctuations in PbPb and pPb collisions, *Phys. Rev. C* 92 (3) (2015) 034911. [arXiv:1503.01692](#), [doi:10.1103/PhysRevC.92.034911](#).
- [92] G. Aad, et al., Measurement of the distributions of event-by-event flow harmonics in lead-lead collisions at $\sqrt{s_{NN}} = 2.76$ TeV with the ATLAS detector at the LHC, *JHEP* 11 (2013) 183. [arXiv:1305.2942](#), [doi:10.1007/JHEP11\(2013\)183](#).
- [93] G. Aad, et al., Measurement of event-plane correlations in $\sqrt{s_{NN}} = 2.76$ TeV lead-lead collisions with the ATLAS detector, *Phys. Rev. C* 90 (2) (2014) 024905. [arXiv:1403.0489](#), [doi:10.1103/PhysRevC.90.024905](#).
- [94] G. Aad, et al., Measurement of the correlation between flow harmonics of different order in lead-lead collisions at $\sqrt{s_{NN}} = 2.76$ TeV with the ATLAS detector, *Phys. Rev. C* 92 (3) (2015) 034903. [arXiv:1504.01289](#), [doi:10.1103/PhysRevC.92.034903](#).
- [95] J. Adam, et al., Correlated event-by-event fluctuations of flow harmonics in PbPb collisions at $\sqrt{s_{NN}} = 2.76$ TeV, *Phys. Lett. B* 753 (2016) 126–139. [arXiv:1604.07663](#).
- [96] J. Adam, et al., Direct photon production in PbPb collisions at $\sqrt{s_{NN}} = 2.76$ TeV, *Phys. Lett. B* 754 (2016) 235–248. [arXiv:1509.07324](#), [doi:10.1016/j.physletb.2016.01.020](#).
- [97] G. Aad, et al., Observation of a centrality-dependent dijet asymmetry in lead-lead collisions at $\sqrt{s_{NN}} = 2.76$ TeV with the ATLAS Detector at the LHC, *Phys. Rev. Lett.* 105 (2010) 252303. [arXiv:1011.6182](#), [doi:10.1103/PhysRevLett.105.252303](#).
- [98] K. Aamodt, et al., Suppression of charged particle production at large transverse momentum in central PbPb collisions at $\sqrt{s_{NN}} = 2.76$ TeV, *Phys. Lett. B* 696 (2011) 30–39. [arXiv:1012.1004](#), [doi:10.1016/j.physletb.2010.12.020](#).
- [99] S. Chatrchyan, et al., Observation and studies of jet quenching in PbPb collisions at nucleon-nucleon center-of-mass energy = 2.76 TeV, *Phys. Rev. C* 84 (2011) 024906. [arXiv:1102.1957](#), [doi:10.1103/PhysRevC.84.024906](#).
- [100] S. Chatrchyan, et al., Study of high- p_T charged particle suppression in PbPb compared to pp collisions at $\sqrt{s_{NN}} = 2.76$ TeV, *Eur. Phys. J. C* 72 (2012) 1945. [arXiv:1202.2554](#), [doi:10.1140/epjc/s10052-012-1945-x](#).
- [101] B. Abelev, et al., Centrality dependence of charged particle production at large transverse momentum in PbPb collisions at $\sqrt{s_{NN}} = 2.76$ TeV, *Phys. Lett. B* 720 (2013) 52–62. [arXiv:1208.2711](#), [doi:10.1016/j.physletb.2013.01.051](#).
- [102] B. Abelev, et al., Suppression of high transverse momentum D mesons in central PbPb collisions at $\sqrt{s_{NN}} = 2.76$ TeV, *JHEP* 09 (2012) 112. [arXiv:1203.2160](#), [doi:10.1007/JHEP09\(2012\)112](#).
- [103] G. Aad, et al., Measurements of the nuclear modification factor for jets in PbPb collisions at $\sqrt{s_{NN}} = 2.76$ TeV with the ATLAS Detector, *Phys. Rev. Lett.* 114 (7) (2015) 072302. [arXiv:1411.2357](#), [doi:10.1103/PhysRevLett.114.072302](#).
- [104] J. Adam, et al., Measurement of jet suppression in central PbPb collisions at $\sqrt{s_{NN}} = 2.76$ TeV, *Phys. Lett. B* 746 (2015) 1–14. [arXiv:1502.01689](#), [doi:10.1016/j.physletb.2015.04.039](#).
- [105] G. Aad, et al., Measurement of charged-particle spectra in PbPb collisions at $\sqrt{s_{NN}} = 2.76$ TeV with the ATLAS detector at the LHC, *JHEP* 09 (2015) 050. [arXiv:1504.04337](#), [doi:10.1007/JHEP09\(2015\)050](#).
- [106] E. Abbas, et al., J/ψ elliptic flow in PbPb collisions at $\sqrt{s_{NN}} = 2.76$ TeV, *Phys. Rev. Lett.* 111 (2013) 162301. [arXiv:1303.5880](#), [doi:10.1103/PhysRevLett.111.162301](#).
- [107] B. Abelev, et al., D meson elliptic flow in non-central PbPb collisions at $\sqrt{s_{NN}} = 2.76$ TeV, *Phys. Rev. Lett.* 111 (2013) 102301. [arXiv:1305.2707](#), [doi:10.1103/PhysRevLett.111.102301](#).
- [108] B. B. Abelev, et al., Azimuthal anisotropy of D meson production in PbPb collisions at $\sqrt{s_{NN}} = 2.76$ TeV, *Phys. Rev. C* 90 (3) (2014) 034904. [arXiv:1405.2001](#), [doi:10.1103/PhysRevC.90.034904](#).
- [109] J. Adam, et al., Elliptic flow of muons from heavy-flavour hadron decays at forward rapidity in PbPb collisions at $\sqrt{s_{NN}} = 2.76$ TeV, *Phys. Lett. B* 753 (2016) 41–56. [arXiv:1507.03134](#), [doi:10.1016/j.physletb.2015.11.059](#).
- [110] B. Abelev, et al., J/ψ suppression at forward rapidity in PbPb collisions at $\sqrt{s_{NN}} = 2.76$ TeV, *Phys. Rev. Lett.* 109 (2012) 072301. [arXiv:1202.1383](#), [doi:10.1103/PhysRevLett.109.072301](#).
- [111] J. Adam, et al., Inclusive, prompt and non-prompt J/ψ production at mid-rapidity in PbPb collisions at $\sqrt{s_{NN}} = 2.76$ TeV, *JHEP* 07 (2015) 051. [arXiv:1504.07151](#), [doi:10.1007/JHEP07\(2015\)051](#).
- [112] S. Chatrchyan, et al., Observation of sequential Upsilon suppression in PbPb collisions, *Phys. Rev. Lett.* 109 (2012) 222301. [arXiv:1208.2826](#), [doi:10.1103/PhysRevLett.109.222301](#).
- [113] S. Chatrchyan, et al., Event activity dependence of $Y(nS)$ production in $\sqrt{s_{NN}} = 5.02$ TeV pPb and $\sqrt{s} = 2.76$ TeV pp collisions, *JHEP* 04 (2014) 103. [arXiv:1312.6300](#), [doi:10.1007/JHEP04\(2014\)103](#).

- [114] B. B. Abelev, et al., Suppression of $\psi(2S)$ production in pPb collisions at $\sqrt{s_{NN}} = 5.02$ TeV, JHEP 12 (2014) 073. arXiv:1405.3796, doi:10.1007/JHEP12(2014)073.
- [115] J. Adam, et al., Centrality dependence of inclusive J/ψ production in pPb collisions at $\sqrt{s_{NN}} = 5.02$ TeV, JHEP 11 (2015) 127. arXiv:1506.08808, doi:10.1007/JHEP11(2015)127.
- [116] J. Adam, et al., Centrality dependence of $\psi(2S)$ suppression in pPb collisions at $\sqrt{s_{NN}} = 5.02$ TeV, JHEP 06 (2016) 050. arXiv:1603.02816, doi:10.1007/JHEP06(2016)050.
- [117] V. Loggins (for the ALICE collaboration), Azimuthally differential pion femtoscopy in PbPb collisions at 2.76 TeV with ALICE at the LHC, Nucl. Phys. A931 (2014) 1088–1092. arXiv:1408.0068, doi:10.1016/j.nuclphysa.2014.08.061.
- [118] M. Krzewicki, Anisotropic flow of identified hadrons in heavy-ion collisions at the LHC, Ph.D. thesis, Utrecht U., CERN-THESIS-2013-306 (2013).
- [119] A. Bilandzic (for the ALICE collaboration), Anisotropic flow analysis in the alice experiment, AIP Conference Proceedings 1343 (1) (2011) 465–467. doi:10.1063/1.3575063.
- [120] M. Wilde (for the ALICE collaboration), Measurement of direct photons in pp and PbPb collisions with ALICE, Nucl. Phys. A904-905 (2013) 573c–576c. arXiv:1210.5958, doi:10.1016/j.nuclphysa.2013.02.079.
- [121] J. Adam, et al., Centrality dependence of particle production in pPb collisions at $\sqrt{s_{NN}} = 5.02$ TeV, Phys. Rev. C91 (6) (2015) 064905. arXiv:1412.6828, doi:10.1103/PhysRevC.91.064905.
- [122] E. Pereira de Oliveira Filho (for the ALICE collaboration), Measurements of electrons from heavy-flavour hadron decays in pp, pPb and PbPb collisions with ALICE at the LHC, Nucl. Phys. A932 (2014) 258–263. arXiv:1404.3983, doi:10.1016/j.nuclphysa.2014.09.069.
- [123] J.-Y. Ollitrault, Anisotropy as a signature of transverse collective flow, Phys. Rev. D46 (1992) 229–245. doi:10.1103/PhysRevD.46.229.
- [124] R. J. Fries, V. Greco, P. Sorensen, Coalescence models for hadron formation from Quark Gluon Plasma, Ann. Rev. Nucl. Part. Sci. 58 (2008) 177–205. arXiv:0807.4939, doi:10.1146/annurev.nucl.58.110707.171134.
- [125] S. Chatrchyan, et al., Study of Z boson production in PbPb collisions at $\sqrt{s_{NN}} = 2.76$ TeV, Phys. Rev. Lett. 106 (2011) 212301. arXiv:1102.5435, doi:10.1103/PhysRevLett.106.212301.
- [126] S. Chatrchyan, et al., Measurement of isolated photon production in pp and PbPb collisions at $\sqrt{s_{NN}} = 2.76$ TeV, Phys. Lett. B710 (2012) 256–277. arXiv:1201.3093, doi:10.1016/j.physletb.2012.02.077.
- [127] S. Chatrchyan, et al., Study of W boson production in PbPb and pp collisions at $\sqrt{s_{NN}} = 2.76$ TeV, Phys. Lett. B715 (2012) 66–87. arXiv:1205.6334, doi:10.1016/j.physletb.2012.07.025.
- [128] G. Aad, et al., Measurement of Z boson production in PbPb collisions at $\sqrt{s_{NN}} = 2.76$ TeV with the ATLAS Detector, Phys. Rev. Lett. 110 (2) (2013) 022301. arXiv:1210.6486, doi:10.1103/PhysRevLett.110.022301.
- [129] S. Chatrchyan, et al., Study of Z production in PbPb and pp collisions at $\sqrt{s_{NN}} = 2.76$ TeV in the dimuon and dielectron decay channels, JHEP 03 (2015) 022. arXiv:1410.4825, doi:10.1007/JHEP03(2015)022.
- [130] G. Aad, et al., Measurement of the production and lepton charge asymmetry of W bosons in PbPb collisions at $\sqrt{s_{NN}} = 2.76$ TeV with the ATLAS detector, Eur. Phys. J. C75 (1) (2015) 23. arXiv:1408.4674, doi:10.1140/epjc/s10052-014-3231-6.
- [131] G. Aad, et al., Centrality, rapidity and transverse momentum dependence of isolated prompt photon production in lead-lead collisions at $\sqrt{s_{NN}} = 2.76$ TeV measured with the ATLAS detector arXiv:1506.08552.
- [132] S. Chatrchyan, et al., Measurement of jet fragmentation in PbPb and pp collisions at $\sqrt{s_{NN}} = 2.76$ TeV, Phys. Rev. C90 (2) (2014) 024908. arXiv:1406.0932, doi:10.1103/PhysRevC.90.024908.
- [133] G. Aad, et al., Measurement of inclusive jet charged-particle fragmentation functions in PbPb collisions at $\sqrt{s_{NN}} = 2.76$ TeV with the ATLAS detector, Phys. Lett. B739 (2014) 320–342. arXiv:1406.2979, doi:10.1016/j.physletb.2014.10.065.
- [134] V. Khachatryan, et al., Measurement of transverse momentum relative to dijet systems in PbPb and pp collisions at $\sqrt{s_{NN}} = 2.76$ TeV, JHEP 01 (2016) 006. arXiv:1509.09029, doi:10.1007/JHEP01(2016)006.
- [135] D. Lohner (for the ALICE collaboration), Measurement of direct-photon elliptic flow in PbPb collisions at $\sqrt{s_{NN}} = 2.76$ TeV, J. Phys. Conf. Ser. 446 (2013) 012028. arXiv:1212.3995, doi:10.1088/1742-6596/446/1/012028.
- [136] S. Chatrchyan, et al., Studies of azimuthal dihadron correlations in ultra-central PbPb collisions at $\sqrt{s_{NN}} = 2.76$ TeV, JHEP 02 (2014) 088. arXiv:1312.1845, doi:10.1007/JHEP02(2014)088.
- [137] J. Adam, et al., Multipion Bose-Einstein correlations in pp, pPb, and PbPb collisions at the LHC arXiv:1512.08902.
- [138] E. Shuryak, I. Zahed, High-multiplicity pp and pA collisions: Hydrodynamics at its edge, Phys. Rev. C88 (4) (2013) 044915. arXiv:1301.4470, doi:10.1103/PhysRevC.88.044915.
- [139] A. Bilandzic, R. Snellings, S. Voloshin, Flow analysis with cumulants: Direct calculations, Phys. Rev. C83 (2011) 044913. arXiv:1010.0233, doi:10.1103/PhysRevC.83.044913.
- [140] R. S. Bhalerao, N. Borghini, J. Y. Ollitrault, Analysis of anisotropic flow with Lee-Yang zeroes, Nucl. Phys. A727 (2003) 373–426. arXiv:nucl-th/0310016, doi:10.1016/j.nuclphysa.2003.08.007.
- [141] T. Sjöstrand, S. Mrenna, P. Skands, Pythia 6.4 physics and manual, Journal of High Energy Physics 2006 (05) (2006) 026.
- [142] J. Jia, S. Radhakrishnan, Limitation of multiparticle correlations for studying the event-by-event distribution of harmonic flow in heavy-ion collisions, Phys. Rev. C92 (2) (2015) 024911. arXiv:1412.4759, doi:10.1103/PhysRevC.92.024911.
- [143] M. Gyulassy, P. Levai, I. Vitev, T. S. Biro, Non-Abelian bremsstrahlung and azimuthal asymmetries in high energy pA reactions, Phys. Rev. D90 (5) (2014) 054025. arXiv:1405.7825, doi:10.1103/PhysRevD.90.054025.
- [144] L. McLerran, V. V. Skokov, The eccentric collective BFKL pomeron, Acta Phys. Polon. B46 (8) (2015) 1513. arXiv:1407.2651, doi:10.5506/APhysPolB.46.1513.
- [145] C. Shen, U. Heinz, P. Huovinen, H. Song, Radial and elliptic flow in PbPb collisions at the Large Hadron Collider from viscous hydrodynamic, Phys. Rev. C84 (2011) 044903. arXiv:1105.3226, doi:10.1103/PhysRevC.84.044903.
- [146] G. Aad, et al., Centrality and rapidity dependence of inclusive jet production in $\sqrt{s_{NN}} = 5.02$ TeV pPb collisions with the ATLAS detector, Phys. Lett. B748 (2015) 392–413. arXiv:1412.4092, doi:10.1016/j.physletb.2015.07.023.

- [147] S. Chatrchyan, et al., Studies of dijet transverse momentum balance and pseudorapidity distributions in pPb collisions at $\sqrt{s_{NN}} = 5.02$ TeV, *Eur. Phys. J. C* 74 (7) (2014) 2951. [arXiv:1401.4433](#), [doi:10.1140/epjc/s10052-014-2951-y](#).
- [148] J. Adam, et al., Measurement of D-meson production versus multiplicity in pPb collisions at $\sqrt{s_{NN}} = 5.02$ TeV [arXiv:1602.07240](#).
- [149] G. Aad, et al., Measurement of the centrality dependence of the charged-particle pseudorapidity distribution in proton-lead collisions at $\sqrt{s_{NN}} = 5.02$ TeV with the ATLAS detector [arXiv:1508.00848](#).
- [150] B. Abelev, et al., Multiplicity dependence of jet-like two-particle correlation structures in pPb collisions at $\sqrt{s_{NN}} = 5.02$ TeV, *Phys. Lett. B* 741 (2015) 38–50. [arXiv:1406.5463](#), [doi:10.1016/j.physletb.2014.11.028](#).
- [151] C. Collaboration, Jet fragmentation function in pPb collisions at $\sqrt{s_{NN}} = 5.02$ TeV and pp collisions at $\sqrt{s} = 2.76$ and 7 TeV, CMS-PAS-HIN-15-004.
- [152] J. Adam, et al., Centrality dependence of charged jet production in pPb collisions at $\sqrt{s_{NN}} = 5.02$ TeV, *Eur. Phys. J. C* 76 (5) (2016) 271. [arXiv:1603.03402](#), [doi:10.1140/epjc/s10052-016-4107-8](#).
- [153] J. Adam, et al., Measurement of dijet k_T in pPb collisions at $\sqrt{s_{NN}} = 5.02$ TeV, *Phys. Lett. B* 746 (2015) 385–395. [arXiv:1503.03050](#), [doi:10.1016/j.physletb.2015.05.033](#).
- [154] C. Shen, C. Park, J.-F. Paquet, G. S. Denicol, S. Jeon, C. Gale, Direct photon production and jet energy-loss in small systems (2016) these proceedings [arXiv:1601.03070](#).
- [155] B. Schenke, S. Schlichting, R. Venugopalan, Azimuthal anisotropies in pPb collisions from classical Yang–Mills dynamics, *Phys. Lett. B* 747 (2015) 76–82. [arXiv:1502.01331](#), [doi:10.1016/j.physletb.2015.05.051](#).
- [156] T. Kalaydzhyan, E. Shuryak, Collective flow in high-multiplicity proton-proton collisions, *Phys. Rev. C* 91 (5) (2015) 054913. [arXiv:1503.05213](#), [doi:10.1103/PhysRevC.91.054913](#).
- [157] A. Ortiz Velasquez, P. Christiansen, E. Cuautle Flores, I. Maldonado Cervantes, G. Paic, Color reconnection and flowlike patterns in pp collisions, *Phys. Rev. Lett.* 111 (4) (2013) 042001. [arXiv:1303.6326](#), [doi:10.1103/PhysRevLett.111.042001](#).
- [158] B. Abelev, et al., Multiplicity dependence of the average transverse momentum in pp, pPb, and PbPb collisions at the LHC, *Phys. Lett. B* 727 (2013) 371–380. [arXiv:1307.1094](#), [doi:10.1016/j.physletb.2013.10.054](#).
- [159] J. Adam, et al., Multiplicity and transverse momentum evolution of charge-dependent correlations in pp, pPb and PbPb collisions at the LHC [arXiv:1509.07255](#).
- [160] Y. Hirono, E. Shuryak, Femtoscopic signature of strong radial flow in high-multiplicity pp collisions, *Phys. Rev. C* 91 (5) (2015) 054915. [arXiv:1412.0063](#), [doi:10.1103/PhysRevC.91.054915](#).
- [161] V. Khachatryan, et al., Measurement of long-range near-side two-particle angular correlations in pp collisions at $\sqrt{s} = 13$ TeV, *Phys. Rev. Lett.* 116 (17) (2016) 172302. [arXiv:1510.03068](#), [doi:10.1103/PhysRevLett.116.172302](#).
- [162] K. Aamodt, et al., Centrality dependence of the charged-particle multiplicity density at mid-rapidity in PbPb collisions at $\sqrt{s_{NN}} = 2.76$ TeV, *Phys. Rev. Lett.* 106 (2011) 032301. [arXiv:1012.1657](#), [doi:10.1103/PhysRevLett.106.032301](#).
- [163] B. Alver, et al., Phobos results on charged particle multiplicity and pseudorapidity distributions in AuAu, CuCu, dAu, and pp collisions at ultra-relativistic energies, *Phys. Rev. C* 83 (2011) 024913. [arXiv:1011.1940](#), [doi:10.1103/PhysRevC.83.024913](#).
- [164] B. Abelev, et al., Multiplicity dependence of two-particle azimuthal correlations in pp collisions at the LHC, *JHEP* 09 (2013) 049. [arXiv:1307.1249](#), [doi:10.1007/JHEP09\(2013\)049](#).
- [165] G. Torrieri, Origin of long-range azimuthal correlations in hadronic collisions, *Phys. Rev. C* 89 (2) (2014) 024908. [arXiv:1310.3529](#), [doi:10.1103/PhysRevC.89.024908](#).
- [166] B. G. Zakharov, Parton energy loss in the mini quark-gluon plasma and jet quenching in proton-proton collisions, *J. Phys. G* 41 (2014) 075008. [arXiv:1311.1159](#), [doi:10.1088/0954-3889/41/7/075008](#).
- [167] B. Abelev, et al., Underlying Event measurements in pp collisions at $\sqrt{s} = 0.9$ and 7 TeV with the ALICE experiment at the LHC, *JHEP* 07 (2012) 116. [arXiv:1112.2082](#), [doi:10.1007/JHEP07\(2012\)116](#).
- [168] B. Abelev, et al., J/ψ production as a function of charged particle multiplicity in pp collisions at $\sqrt{s} = 7$ TeV, *Phys. Lett. B* 712 (2012) 165–175. [arXiv:1202.2816](#), [doi:10.1016/j.physletb.2012.04.052](#).
- [169] H. Leon Vargas (for the ALICE collaboration), Connecting the underlying event with jet properties in pp collisions at $\sqrt{s} = 7$ TeV with the ALICE experiment, *J. Phys. Conf. Ser.* 389 (2012) 012004. [arXiv:1208.0940](#), [doi:10.1088/1742-6596/389/1/012004](#).
- [170] J. Adam, et al., Measurement of charm and beauty production at central rapidity versus charged-particle multiplicity in proton-proton collisions at $\sqrt{s} = 7$ TeV, *JHEP* 09 (2015) 148. [arXiv:1505.00664](#), [doi:10.1007/JHEP09\(2015\)148](#).
- [171] G. Aad, et al., Measurement of the dependence of transverse energy production at large pseudorapidity on the hard-scattering kinematics of pp collisions at $\sqrt{s} = 2.76$ TeV with ATLAS [arXiv:1512.00197](#).
- [172] K. Dusling, W. Li, B. Schenke, Novel collective phenomena in high-energy proton-proton and proton-nucleus Collisions [arXiv:1509.07939](#).
- [173] M. Gyulassy, L. McLerran, New forms of QCD matter discovered at RHIC, *Nucl. Phys. A* 750 (2005) 30–63. [arXiv:nuc1-th/0405013](#), [doi:10.1016/j.nuclphysa.2004.10.034](#).
- [174] C. Shen, U. Heinz, The road to precision: Extraction of the specific shear viscosity of the quark-gluon plasma [arXiv:1507.01558](#).
- [175] G. Başar, D. Teaney, Scaling relation between pA and A collisions, *Phys. Rev. C* 90 (5) (2014) 054903. [arXiv:1312.6770](#), [doi:10.1103/PhysRevC.90.054903](#).
- [176] E. V. Shuryak, O. V. Zhironov, Vacuum pressure effects in low p_T hadronic spectra, *Phys. Lett. B* 89 (1979) 253–255. [doi:10.1016/0370-2693\(80\)90023-4](#).
- [177] P. Bozek, Small systems - hydrodynamics (2016) these proceedings.
- [178] E. Avsar, C. Flensburg, Y. Hatta, J.-Y. Ollitrault, T. Ueda, Eccentricity and elliptic flow in proton-proton collisions from parton

- evolution, Phys. Lett. B702 (2011) 394–397. [arXiv:1009.5643](#), doi:10.1016/j.physletb.2011.07.031.
- [179] J. Casalderrey-Solana, U. A. Wiedemann, Eccentricity fluctuations make flow measurable in high multiplicity pp collisions, Phys. Rev. Lett. 104 (2010) 102301. [arXiv:0911.4400](#), doi:10.1103/PhysRevLett.104.102301.
- [180] A. Bzdak, B. Schenke, P. Tribedy, R. Venugopalan, Initial state geometry and the role of hydrodynamics in proton-proton, proton-nucleus and deuteron-nucleus collisions, Phys. Rev. C87 (6) (2013) 064906. [arXiv:1304.3403](#), doi:10.1103/PhysRevC.87.064906.
- [181] H. Heiselberg, A.-M. Levy, Elliptic flow and HBT in noncentral nuclear collisions, Phys. Rev. C59 (1999) 2716–2727. [arXiv:nuc1-th/9812034](#), doi:10.1103/PhysRevC.59.2716.
- [182] J. Adam, et al., Pseudorapidity and transverse-momentum distributions of charged particles in proton–proton collisions at $\sqrt{s} = 13$ TeV, Phys. Lett. B753 (2016) 319–329. [arXiv:1509.08734](#), doi:10.1016/j.physletb.2015.12.030.
- [183] B. Alver, et al., System size, energy, pseudorapidity, and centrality dependence of elliptic flow, Phys. Rev. Lett. 98 (2007) 242302. [arXiv:nuc1-ex/0610037](#), doi:10.1103/PhysRevLett.98.242302.
- [184] B. Alver, et al., Non-flow correlations and elliptic flow fluctuations in gold-gold collisions at $\sqrt{s_{NN}} = 200$ GeV, Phys. Rev. C81 (2010) 034915. [arXiv:1002.0534](#), doi:10.1103/PhysRevC.81.034915.
- [185] B. Alver, G. Roland, Collision geometry fluctuations and triangular flow in heavy-ion collisions, Phys. Rev. C81 (2010) 054905, [Erratum: Phys. Rev.C82,039903(2010)]. [arXiv:1003.0194](#), doi:10.1103/PhysRevC.82.039903, doi:10.1103/PhysRevC.81.054905.
- [186] A. Adare, et al., Measurements of elliptic and triangular flow in high-multiplicity $^3\text{HeAu}$ collisions at $\sqrt{s_{NN}} = 200$ GeV, Phys. Rev. Lett. 115 (14) (2015) 142301. [arXiv:1507.06273](#), doi:10.1103/PhysRevLett.115.142301.
- [187] J. Nagle, A. Adare, S. Beckman, T. Koblesky, J. O. Koop, D. McGlinchey, P. Romatschke, J. Carlson, J. Lynn, M. McCumber, Exploiting intrinsic triangular geometry in relativistic $^3\text{HeAu}$ collisions to disentangle medium properties, Phys. Rev. Lett. 113 (11) (2014) 112301. [arXiv:1312.4565](#), doi:10.1103/PhysRevLett.113.112301.
- [188] Z. Xu, C. Greiner, Thermalization of gluons in ultrarelativistic heavy ion collisions by including three-body interactions in a parton cascade, Phys. Rev. C71 (2005) 064901. [arXiv:hep-ph/0406278](#), doi:10.1103/PhysRevC.71.064901.
- [189] Z.-W. Lin, C. M. Ko, B.-A. Li, B. Zhang, S. Pal, A Multi-phase transport model for relativistic heavy ion collisions, Phys. Rev. C72 (2005) 064901. [arXiv:nuc1-th/0411110](#), doi:10.1103/PhysRevC.72.064901.
- [190] D. Molnar, M. Gyulassy, Saturation of elliptic flow and the transport opacity of the gluon plasma at RHIC, Nucl. Phys. A697 (2002) 495–520, [Erratum: Nucl. Phys.A703,893(2002)]. [arXiv:nuc1-th/0104073](#), doi:10.1016/S0375-9474(01)01224-6.
- [191] Z.-W. Lin, Evolution of transverse flow and effective temperatures in the parton phase from a multi-phase transport model, Phys. Rev. C90 (1) (2014) 014904. [arXiv:1403.6321](#), doi:10.1103/PhysRevC.90.014904.
- [192] G.-L. Ma, A. Bzdak, Long-range azimuthal correlations in proton-proton and proton-nucleus collisions from the incoherent scattering of partons, Phys. Lett. B739 (2014) 209–213. [arXiv:1404.4129](#), doi:10.1016/j.physletb.2014.10.066.
- [193] A. Bzdak, G.-L. Ma, Elliptic and triangular flow in pPb and peripheral PbPb collisions from parton scatterings, Phys. Rev. Lett. 113 (25) (2014) 252301. [arXiv:1406.2804](#), doi:10.1103/PhysRevLett.113.252301.
- [194] G.-L. Ma, Z.-W. Lin, Predictions for $\sqrt{s_{NN}} = 5.02$ TeV PbPb collisions from a Multi-Phase Transport Model [arXiv:1601.08160](#).
- [195] L. He, T. Edmonds, Z.-W. Lin, F. Liu, D. Molnar, F. Wang, Anisotropic parton escape is the dominant source of azimuthal anisotropy in transport models, Phys. Lett. B753 (2016) 506–510. [arXiv:1502.05572](#), doi:10.1016/j.physletb.2015.12.051.
- [196] Z.-W. Lin, L. He, T. Edmonds, F. Liu, D. Molnar, F. Wang, Elliptic Anisotropy v_2 May Be Dominated by Particle Escape instead of Hydrodynamic Flow (2015) these proceedings [arXiv:1512.06465](#).
- [197] H. Li, L. He, Z.-W. Lin, D. Molnar, F. Wang, W. Xie, Origin of the mass splitting of elliptic anisotropy in A Multi-Phase Transport model [arXiv:1601.05390](#).
- [198] P. Romatschke, Collective flow without hydrodynamics: simulation results for relativistic ion collisions, Eur. Phys. J. C75 (9) (2015) 429. [arXiv:1504.02529](#), doi:10.1140/epjc/s10052-015-3646-8.
- [199] P. Romatschke, Small systems - hydrodynamics (2016) these proceedings.
- [200] J. D. O. Koop, R. Belmont, P. Yin, J. L. Nagle, Exploring the beam energy dependence of flow-like signatures in small system dAu collisions [arXiv:1512.06949](#).
- [201] K. Dusling, P. Tribedy, R. Venugopalan, Energy dependence of the ridge in high multiplicity proton-proton collisions, Phys. Rev. D93 (1) (2016) 014034. [arXiv:1509.04410](#), doi:10.1103/PhysRevD.93.014034.
- [202] B. Schenke, S. Schlichting, P. Tribedy, R. Venugopalan, Mass ordering of spectra from fragmentation of saturated gluon states in high multiplicity proton-proton collisions [arXiv:1607.02496](#).
- [203] T. Lappi, B. Schenke, S. Schlichting, R. Venugopalan, Tracing the origin of azimuthal gluon correlations in the color glass condensate, JHEP 01 (2016) 061. [arXiv:1509.03499](#), doi:10.1007/JHEP01(2016)061.
- [204] A. Dumitru, L. McLerran, V. Skokov, Azimuthal asymmetries and the emergence of “collectivity” from multi-particle correlations in high-energy pA collisions, Phys. Lett. B743 (2015) 134–137. [arXiv:1410.4844](#), doi:10.1016/j.physletb.2015.02.046.
- [205] T. Lappi, Azimuthal harmonics of color fields in a high energy nucleus, Phys. Lett. B744 (2015) 315–319. [arXiv:1501.05505](#), doi:10.1016/j.physletb.2015.04.015.
- [206] A. Esposito, M. Gyulassy, Hadronization scheme dependence of long-range azimuthal harmonics in high energy pA reactions, Phys. Lett. B747 (2015) 433–440. [arXiv:1505.03734](#), doi:10.1016/j.physletb.2015.06.037.
- [207] P. Bozek, A. Bzdak, V. Skokov, The rapidity dependence of the average transverse momentum in pPb collisions at the LHC: the Color Glass Condensate versus hydrodynamics, Phys. Lett. B728 (2014) 662–665. [arXiv:1309.7358](#), doi:10.1016/j.physletb.2013.12.034.

- [208] P. Bozek, A. Bzdak, G.-L. Ma, Rapidity dependence of elliptic and triangular flow in proton–nucleus collisions from collective dynamics, *Phys. Lett. B* 748 (2015) 301–305. [arXiv:1503.03655](#), [doi:10.1016/j.physletb.2015.06.007](#).
- [209] S. Schlichting, Initial state and pre-equilibrium effects in small systems (2016) these proceedings [arXiv:1601.01177](#).